Article

Bull. Volcanol. Soc. Japan
Vol. 58 (2013) No. 1, pp. 191−212

Temporal Variations of the Petrological Features of the Juvenile Materials during 2006 to 2010 from Showa Crater, Sakurajima Volcano, Kyushu, Japan

Akiko Matsumoto*, Mitsuhiro Nakagawa*, Mizuho Amma-Miyasaka* and Masato Iguchi**

(Received August 19, 2011; Accepted February 10, 2012)

On June 2006, Sakurajima volcano in Japan resumed its eruptive activity at Showa crater in Minamidake. We investigated dated ash samples, including lapilli ejecta of several eruptions, to evaluate the temporal relationship between their petrological features and eruptive activity. The activity is characterized by low frequency of explosive eruptions accompanied with small, periodic inflation from June 2006 to August 2009. No juvenile materials existed in the ash during this period (1st period). Frequent explosive eruptions accompanied with large, continuous inflation had continued from September 2009 until March 2010 (2nd period). Juvenile materials such as unaltered scoria and pumice with fresh glass have been recognized since late September 2009. The whole-rock chemistry of these juvenile materials is similar to those from AD 1955 to AD 2000 but is the most mafic (SiO_2＝58.5−59.1 wt.%), indicating that the magma system, in which mafic magma was injected into silicic magma, has not changed. The matrix glass compositions of the juvenile materials are dacitic (SiO_2＝67.2−72.7 wt.%). During the 2nd period, the proportion of juvenile materials in eruptive ash increased and the SiO_2 contents of glass decreased with time. These temporal changes suggest that the high level of eruptive activity during the 2nd period was caused by the increase of mafic components in eruptive magma. During April to May 2010 (3rd period), the number of eruption had become small without inflation, and the proportion of juvenile materials also decreased. From June 2010 (4th period), although the mode of crustal deformation has changed to deflation, eruptive activity has increased again and the juvenile materials have been mainly ejected. The glass compositions during this period have become slightly higher in SiO_2 content. These temporal changes of eruptive style and glass compositions suggest that the eruptive activity since AD 2006 has not been directly affected by the addition of mafic components in the magma system, but has occurred because of the silicic (andesitic) magma already-supplied beneath the volcano. In this way, the monitoring of the petrological features of dated eruptive materials could provide us useful information to evaluate ongoing eruptive activity as well as geophysical monitoring.

Key words: Sakurajima volcano, volcanic ash, Showa crater, juvenile material, temporal variation

1. Introduction

Sakurajima volcano, located in southern Kyushu, is one of the most active volcanoes in Japan (Fig. 1). Four large historical eruptions have been recorded at Sakurajima (AD 764−766, AD 1471−1476, AD 1779, and AD 1914−1915), in each of which vigorous lava flows had effused after a plinian eruption (Fukuyama and Ono, 1981; Kobayashi, 1982; Kobayashi and Ishihara, 1988). After the AD 1914−1915 eruption, the eruptive style of the volcano changed. Small scale of eruptions occurred at the east-southeast flank of Minamidake during AD 1935−1945, followed by lava effusion in AD 1946 from Showa crater, which is situated on the eastern slope of Minamidake, ca. 500 meters southeast of Minamidake crater (Fig. 1). Since AD 1955, small but explosive eruptions (vulcanian explosions) have frequently occurred at Minamidake crater. The number of explosive eruptions increased especially in the AD 1970s and 1980s. In the 21st century, however, the frequency of explosions has decreased drastically (Iguchi *et al*., 2008b).

On June 2006, a small phreatic eruption occurred at Showa crater. Thereafter, small eruptions intermittently took place until AD 2008. Since AD 2009, explosive eruptions have often occurred, and their frequency has been increasing significantly until now. These activities have been monitored by a well-developed geophysical monitoring network in the area of Sakurajima volcano to obtain high-quality data sets (*e.g.*, Iguchi *et al*., 2008a,

*Department of Natural History Sciences, Graduate School of Science, Hokkaido University, N10 W8, Kita-ku, Sapporo 060−0810, Japan.
**Sakurajima Volcano Research Center, Disaster Prevention Research Institute, Kyoto University, 1722−19, Sakurajima Yokoyamacho, Kagoshima 891−1419, Japan.

Corresponding author: Akiko Matsumoto
e-mail: a-matsu@mail.sci.hokudai.ac.jp

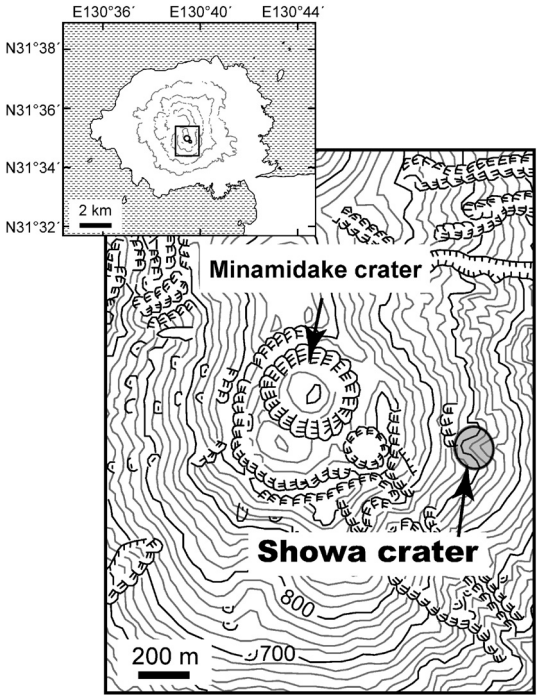

Fig. 1. Locality map of Showa crater of Sakurajima volcano.

2008b; Iguchi, 2010; Iguchi *et al*., 2010; Iguchi *et al*., 2011; Iguchi *et al*., in this issue; Yokoo *et al*., 2009). Although there have been some petrological investigations on volcanic ash from Showa crater since 2006 (Miyagi *et al*., 2010; Shimano *et al*., 2010), we have yet to clarify the petrological features of the juvenile materials produced by the series of eruptions since AD 2006. In this study, we describe the petrological features of dated eruptive materials generated from Showa crater to reveal the characteristics of the erupted magma and its temporal variations. In addition, the relationship between these petrological features and the geophysical data, especially geodesy, is discussed.

2. Volcanic activity at Showa crater during AD 2006 to 2010

At the beginning of the 21st century, the level of eruptive activity at Sakurajima volcano was low (Iguchi *et al*., 2008b; in this issue). However, a small eruption occurred at Showa crater on June 4, 2006, making the resumption of eruptive activity at the crater after 58 years of dormancy. Fig. 2 shows the monthly number of explosions, weight of eruptive ash, and changes of ground deformation.

Small-scale eruptions continued for two weeks to one month in each year from AD 2006 to AD 2007, and explosive eruptions occurred 18 times in AD 2008. Since February 2009, the level of eruptive activity gradually increased. Explosive eruptions were intermittently repeated from February to April 2009 and almost every day from July to September 2009. The number of explosive eruptions in a day has increased considerably since October 2009. The total number of eruptions, accompanied with air shocks, was 896 times in a year until March 2010, according to the monitoring data from the Japan Metrological Agency. However, the eruptive activity suddenly ceased since April 2010. This resumed in the middle of June 2010, and since then explosive eruptions continued until September 2010.

The total weight of erupted volcanic ash was less than 1×10^5 ton/month in AD 2006−2008 when the eruptive activity occurred intermittently (Iguchi, 2010). Since July 2009, the total weight has increased significantly with increasing the number of explosions. The monthly weight of volcanic ash was 6.6×10^5 tons in November 2009 and more than 1×10^6 tons from January to March 2010. However, as the explosive activity became less frequent from April to the middle of June 2010, the weight also decreased during this period ($<5\times10^5$ ton/month). Although the monthly weight of volcanic ash immediately increased again from late June to July 2010 (1×10^6 tons), the weight constantly decreased until September 2010 (less than 4×10^5 tons).

Iguchi *et al*. (2011; in this issue) reported a tilt change in the radial component of the underground tunnel located in the southern area of Sakurajima volcano. Ground deformation related to eruptive activity has been observed. Although small inflation had been observed periodically, the remarkable tilt change had not been detected until AD 2008. After the number of explosions increased in July 2009, clear deflation had been detected. In contrast, continuous inflation had obviously appeared at the end of September 2009 and had continued until early April 2010. The change in ground deformation became much smaller in May 2010. The deflation started after the explosions in the middle of June 2010, and the considerable deflation has been detected until September 2010. The estimated pressure source of the observed ground deformation is located beneath Minamidake at a depth of 4 km (Iguchi, 2011).

3. Sampling, preparation and analytical procedures

The eruptive products were collected around the volcanic edifice in almost real-time since AD 2006 (Table 1). Because the eruptive products in the activity on 2008 and June-August 2010 could not be collected unfortunately, we did not analyze these samples in this study. The collected samples are bimodal in size. Most of the collected samples are ash size (0.1−1 mm), whereas lapilli-size pumice, scoria, and lithic samples (5−30 mm) were also collected on November 17, 2009, and on April 6 and June 12, 2010 (Fig. 3).

All the preparation and analyses for these samples were carried out at Hokkaido University. The samples were

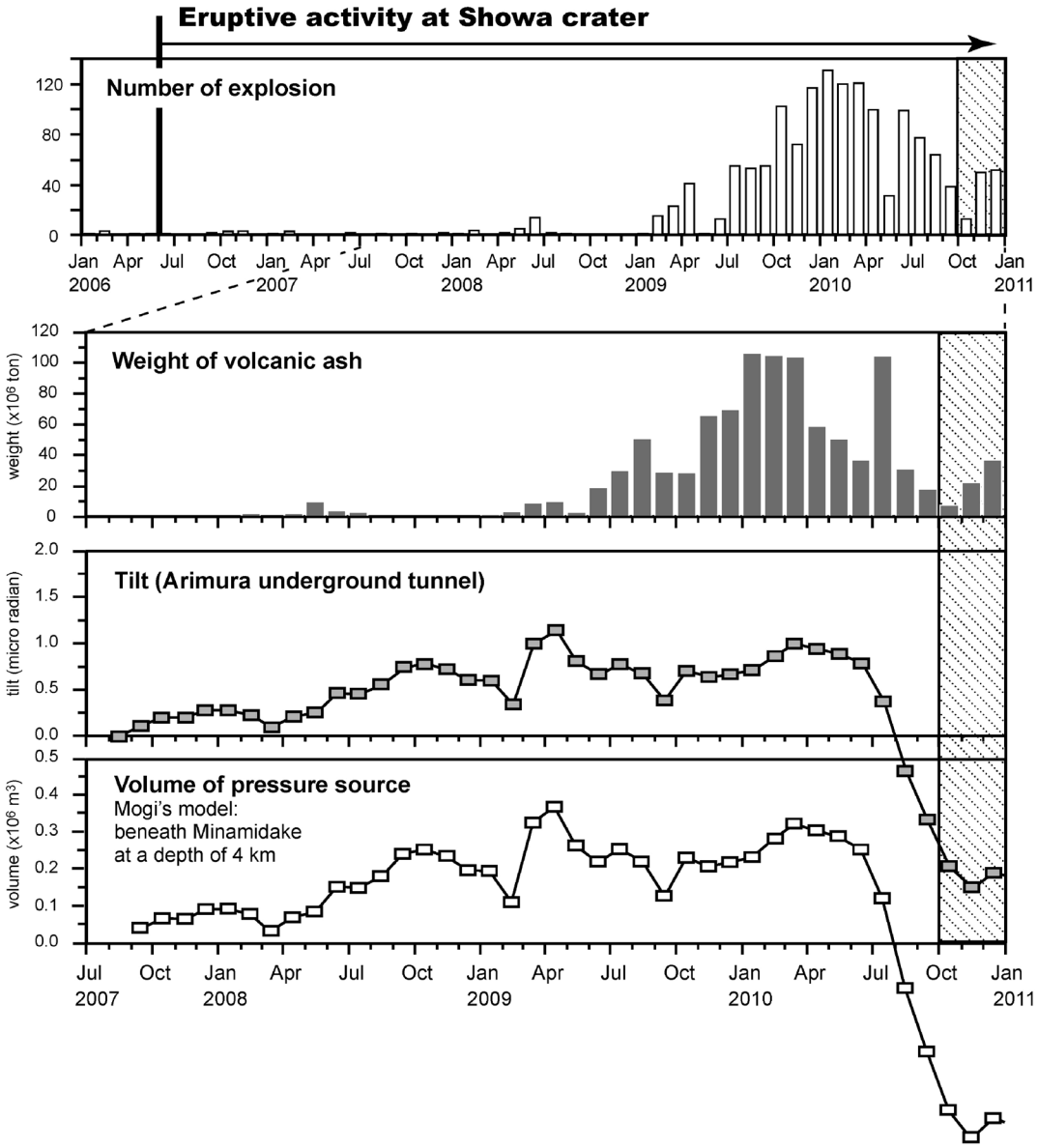

Fig. 2. The monthly variations of geophysical data. Top: number of explosions; Second: weight of volcanic ash; Third and bottom: tilt change at the Arimura underground tunnel (located in the southern area of Sakurajima volcano) and volume of pressure source beneath Minamidake at a depth of 4 km. These data are taken from Iguchi (2010) and Iguchi *et al.* (in this issue). Shaded area shows the non-treated period in this study.

washed using ultrasonic equipment, and thin sections were prepared for microscopic observation. To identify the juvenile materials, we observed the back-scattered electron image (BEI) using a JEOL-8800R electron probe micro-analyser, in addition to the microscopic observation. The juvenile materials represented by lapilli-size pumice and scoria on November 2009 and April 2010 can be identified on the BEIs with the adjusted brightness on plagioclase. Because of this, the glassy materials with the obviously-brighter matrix glass are considered as the juvenile materials from each eruption ("Juvenile-A" type), and the materials showing darker glass are regarded as the magmatic products related to previous eruptions ("Juvenile-B" type). Details are described in Chapter 4.

We carried out the component analysis of ash-size samples on thin section, counting more than 1000 grains

Table 1. Summary of the volcanic ash and lapilli samples generated from Showa crater used in this study.

Sample No.	Eruption Date	Occurrence	Types of Juvenile-A	Collection point (distance and direction from crater)
From Showa crater				
1st period				
Sk-75	6-Jun-2006	ash	-	3.4 km; SW
Sk-070531	31-May-2007	ash	-	1.7 km; S
Sk-070606	6-Jun-2007	ash	-	3 km; WNW
Sk-129	2-Feb-2009	ash	-	3.9 km; SSW
Sk-130	2-Mar-2009	ash	-	3 km; WNW
Sk-131	2-Mar-2009	ash	-	2.6 km; S
Sk-133	2-Apr-2009	ash	-	1.7 km; S
Sk-090505	5-May-2009	ash	-	3.4 km; SW
Sk-090804	4-Aug-2009	ash	-	5.8 km; W
Sk-134	17-Aug-2009	ash	-	5.8 km; W
2nd period				
Sk-090921	21-Sep-2009	ash	scoria, pumice, lithic	2.6 km; S
Sk-091001-1	1-Oct-2009	ash	scoria, pumice	4.9 km; NW
Sk-091001-2	1-Oct-2009	ash	scoria, pumice	3.5 km; SE
Sk-135	21-Oct-2009	ash	scoria, lithic, pumice	5.8 km; W
Sk-136	23-Oct-2009	ash	scoria, pumice, lithic	5.8 km; W
Sk-137	30-Oct-2009	ash	scoria, pumice, lithic	5.8 km; W
Sk-138	8-Nov-2009	ash	scoria, pumice, lithic	5.8 km; W
Sk-126	17-Nov-2009	lapilli	(scoria, lithic)	2.6 km; S
Sk-127	17-Nov-2009	lapilli	(scoria)	2.6 km; S
Sk-128	17-Nov-2009	lapilli	scoria, (lithic)	2.6 km; S
Sk-139	2-Dec-2009	ash	scoria, lithic, pumice	5.8 km; W
Sk-140	6-Jan-2010	ash	scoria, pumice, lithic	2.6 km; S
Sk-141	19-Jan-2010	ash	scoria, pumice, lithic	5.8 km; W
Sk-142	8-Feb-2010	ash	scoria, pumice, lithic	5.8 km; W
Sk-143	19-Feb-2010	ash	scoria, pumice, lithic	2.6 km; S
Sk-144	22-Feb-2010	ash	lithic, scoria	3.6 km; E
Sk-145	8-Mar-2010	ash	scoria, lithic, pumice	5.8 km; W
Sk-146	18-Mar-2010	ash	lithic, scoria, pumice	3.6 km; E
Sk-147	18-Mar-2010	ash	lithic, scoria, pumice	3.6 km; E
Sk-148	18-Mar-2010	ash	scoria, lithic, pumice	3.6 km; E
Sk-149	19-Mar-2010	ash	scoria, lithic, pumice	3.6 km; E
Sk-150	19-Mar-2010	ash	lithic, scoria, pumice	3.5 km; SE
3rd period				
Sk-151-1	6-Apr-2010	ash	pumice, scoria, lithic	1.9 km; ENE
Sk-151-2	6-Apr-2010	lapilli	pumice, scoria, (lithic)	1.9 km; ENE
Sk-152	12-May-2010	ash	pumice, scoria, lithic	4.3 km; SW
Sk-153	12-May-2010	ash	pumice, scoria, lithic	4.3 km; SW
4th period				
Sk-154	12-Jun-2010	lapilli	(scoria, lithic)	2.6 km; S
Sk-157	27-Aug-2010	ash	pumice, scoria, lithic	10.0 km; W
Sk-158	3-Sep-2010	ash	pumice, scoria, lithic	10.0 km; W
Sk-159	3-Sep-2010	ash	scoria, pumice, lithic	10.0 km; W
Sk-160	4-Sep-2010	ash	pumice, scoria, lithic	10.0 km; W
Sk-161	4-Sep-2010	ash	pumice, scoria, lithic	10.0 km; W
Sk-155	13-Sep-2010	ash	pumice, scoria, lithic	8.6 km; W
Sk-156	13-Sep-2010	ash	pumice, scoria, lithic	5.8 km; W

For lapilli samples, the components provided in the parentheses are Juvenile-B types.

per thin section. For the calculation of the proportion of the Juvenile-A type, we also counted these grains on the BEIs. The modal compositions of microlite in the representative high-Si and low-Si Juvenile-A type materials were determined on the BEIs (at 500−1000 magnification). The areas of microlite and interstitial glass were measured using an image processing software package (Image J). We determined the whole-rock compositions of representative volcanic ash as well as lapilli-size samples by an X-ray fluorescence (XRF) using a Spectris MagiX PRO system with Rh tube. A few clasts of lapilli-size materials were powdered as one sample, and the bulk samples of volcanic ash with and without washing were also analyzed. The matrix glass compositions (interstitial glass) were determined using a JEOL-8800R electron probe micro-analyser (WDS). The operating conditions were 15 kV accelerating voltage and 10 nA beam current using a 10 μm beam. All the analyses were corrected by a ZAF cor-

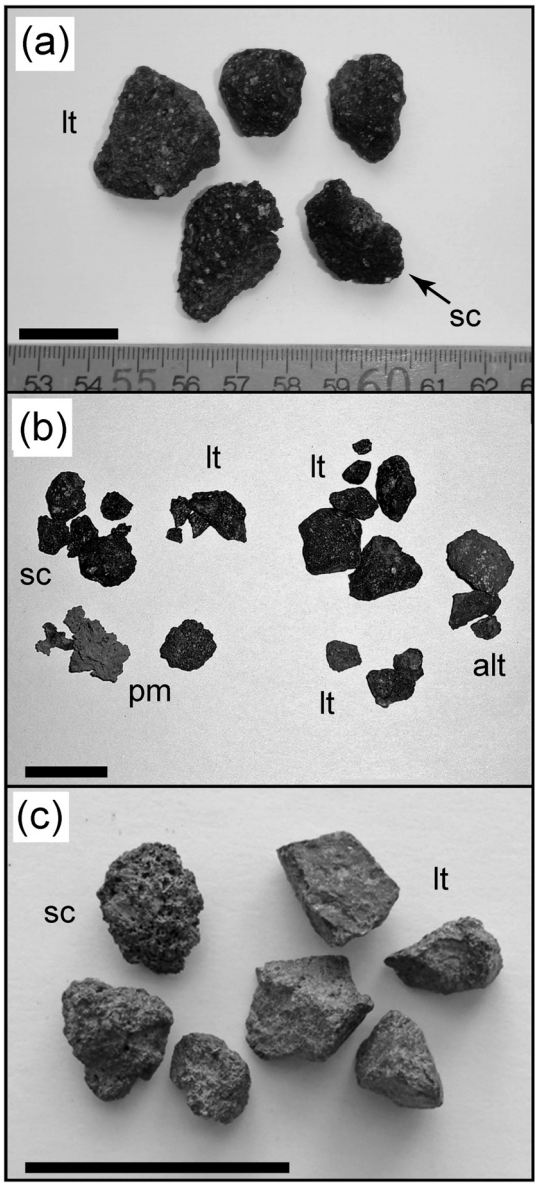

Fig. 3. Photographs of lapilli-size materials from three eruptions at Showa crater. (a) November 17, 2009; (b) April 6, 2010; and (c) June 12, 2010. The boldfaced bars in each photograph represent 2 cm. Abbreviations: lt, lithic; sc, scoria; pm, pumice; and alt: altered material (reddish lithics). There are some strongly altered, reddish lithics (probably high temperature oxidation) in the samples from the April 6, 2010 eruption, whereas most of the lapilli are fresh specimens.

rection method. The matrix glass and whole-rock compositions of the representative samples are listed in Table 2.

4. Petrographical features of eruptive products

On the basis of microscopic and BEI (back-scattered electron image) observations, ash- and lapilli-size samples can be grouped into several types, as described below. The previous study reported that the BEIs were useful for the identification of altered materials (Miyagi and Tomiya, 2002). In addition, they determined the juveniles on the basis of the compositions of magnetite microphenocrysts. In contrast, many ash-size samples in this study don't include magnetite microphenocrysts. Therefore, we recognized the possible juvenile materials among eruptive materials in each eruption on the basis of the brightness on the BEIs (adjusted brightness on plagioclase) in addition to the petrographical features under microscopy.

4−1 Volcanic ash

The volcanic ash, ranging from 0.2 to 0.8 mm in average size, comprises four types of materials: Juvenile-A, Juvenile-B, strongly altered materials, and isolated crystals. The petrographical features of these are as follows:

(a) Juvenile-A type: These materials, including pumice, scoria, and dense lithics (Figs. 4a-c), show an angular shape and are intersertal in texture. Their matrixes are composed mainly of plagioclase, with small amounts of pigeonite and magnetite, and colorless or brown glass. Pumice and scoria are well vesiculated and include a smaller amount of microlite in their matrix compared with those in dense lithics. Regardless of the type of material, the matrix glass is light-colored on the BEIs, and therefore the plagioclase microlites are clearly distinguishable from matrix glass (Figs. 4a-c). According to these features, this type of materials can be considered as juvenile ejecta in each eruption.

(b) Juvenile-B type: These materials are similar to Juvenile-A types in shape and texture on microscopy (Figs. 4d-e). However, their matrix glass is dull-colored and sometimes shows a small amount of silica minerals. On the BEIs, these materials have more microlites and darker matrix glass compared with those of Juvenile-A types, similar to plagioclase on brightness. The matrix glass of these materials usually shows more silicic compositions than those of Juvenile-A types (Appendix 1). These features suggest that Juvenile-B types are magmatic materials not of each eruption, but probably of the previous eruptions since AD 2006. Many microlites might reflect the slow cooling. We call them "Juvenile-B type" in order to distinguish them from the juvenile materials from eruptions before AD 2006.

(c) Strongly altered type: This type of material is strongly altered, and consists of two subtypes: reddish-to-yellowish lithics and silicified lithics (Figs. 4f-g). The reddish-to-yellowish lithics are usually glassy, and rarely include plagioclase microphenocrysts. Their matrix glasses show much darker than those of juvenile materials since AD 2006 on the BEIs (Fig. 4f). They are clearly different from the Juvenile-A and Juvenile-B types in glass compositions (Appendix 1). The silicified lithics have many

Table 2. Representative matrix glass of Juvenile-A types and whole-rock compositions of the volcanic ash and lapilli samples from Showa crater.

Date	02-Mar-09	08-Nov-09	19-Feb-10	18-Mar-10	06-Apr-10	12-May-10	27-Aug-10	13-Sep-10	17-Nov-09	06-Apr-10	12-Jun-10
Sample No.	Sk-131	Sk-138	Sk-143	Sk-148	Sk-151-1	Sk-152	Sk-157	Sk-155	Sk-128	Sk-151-2	Sk-154-2
Occurrence	ash	ash	ash	ash	ash	ash	ash	ash	lapilli	lapilli	lapilli
Type	-	sc,pm,lt	sc,pm,lt	sc,pm,lt	pm,sc,lt	pm,sc,lt	pm,sc,lt	pm,sc,lt	sc	pm,sc/lt[a]	lt
Period	1st	2nd	2nd	2nd	3rd	3rd	4th	4th	2nd	3rd	4th
Glass composition (wt.%, EPMA)											
SiO_2		70.62	69.96	69.40	69.22	67.92	71.20	70.65	71.24	68.68	
TiO_2		1.03	1.31	0.98	1.20	1.11	0.99	0.84	0.99	1.11	
Al_2O_3		12.65	12.11	12.37	12.43	12.47	12.25	13.34	12.32	12.95	
FeO*		5.29	6.65	5.35	6.52	6.29	5.09	4.28	5.02	6.18	
MnO		0.12	0.15	0.07	0.12	0.14	0.13	0.08	0.11	0.14	
MgO		0.76	0.74	0.83	0.85	1.01	0.69	0.72	0.57	1.04	
CaO		3.15	2.78	2.92	3.43	3.46	2.59	2.75	2.52	3.61	
Na_2O		3.64	3.44	3.01	3.47	3.62	3.98	3.77	3.95	3.56	
K_2O		3.39	3.91	4.46	3.58	3.21	3.50	2.86	3.53	3.02	
P_2O_5		0.33	0.42	0.29	0.35	0.31	0.26	0.32	0.31	0.29	
Total		100.98	101.47	99.68	101.16	99.55	100.67	99.61	100.56	100.58	
Average(100%-normalized)											
SiO_2		69.43	68.89	69.01	68.70	68.95	69.41	70.22	70.07	68.74	70.85
TiO_2		1.05	1.09	1.11	1.07	1.08	1.05	0.97	0.96	1.09	0.99
Al_2O_3		12.62	12.51	12.23	12.67	12.44	12.31	12.49	12.57	12.67	12.04
FeO*		5.50	5.82	6.04	5.88	5.91	5.70	5.22	5.17	5.99	5.15
MnO		0.12	0.13	0.12	0.11	0.12	0.12	0.12	0.12	0.13	0.11
MgO		0.82	0.86	0.81	0.89	0.86	0.80	0.73	0.68	0.89	0.65
CaO		3.29	3.18	3.15	3.42	3.24	3.09	2.89	2.83	3.48	2.62
Na_2O		3.49	3.66	3.57	3.52	3.64	3.71	3.57	3.86	3.56	3.72
K_2O		3.31	3.53	3.64	3.40	3.47	3.51	3.50	3.43	3.13	3.58
P_2O_5		0.37	0.33	0.33	0.32	0.31	0.30	0.29	0.31	0.31	0.29
Total		100.00	100.00	100.00	100.00	100.00	100.00	100.00	100.00	100.00	100.00
Number[b]		21	16	19	17	15	22	25	15	20	10
Bulk composition (wt.%, XRF)[c]											
SiO_2	63.09		60.25	60.54	59.21		60.14		59.97	59.25	59.88
TiO_2	0.78		0.84	0.82	0.87		0.78		0.79	0.79	0.79
Al_2O_3	16.05		15.93	16.40	16.80		16.69		17.53	17.28	17.16
Fe_2O_3	6.86		8.19	7.78	8.38		7.73		7.80	7.93	7.93
MnO	0.13		0.16	0.15	0.16		0.16		0.15	0.16	0.16
MgO	2.60		3.52	3.24	3.44		3.53		3.40	3.48	3.45
CaO	5.35		6.36	6.67	7.05		6.94		7.45	7.57	7.30
Na_2O	2.94		3.12	3.14	3.11		3.11		3.28	3.25	3.25
K_2O	1.64		1.49	1.48	1.36		1.40		1.41	1.37	1.44
P_2O_5	0.15		0.16	0.16	0.16		0.16		0.16	0.16	0.17
Total	99.59		100.02	100.38	100.52		100.61		101.94	101.23	101.54

pm: pumice, sc: scoria, lt: lithic.

a: Glass composition of this sample is taken from pumice and scoria, and bulk composition is from lithic.

b: Numbers are shown the number of analyzed points in each sample.

c: The bulk compositions of the volcanic ash are the data of the bulk samples without washing.

silica minerals (probably cristobalite) in their matrix, showing much lower brightness on the BEIs (Fig. 4 g). These are so-called accessory and accidental ejecta.

(d) Isolated crystals: Plagioclase, orthopyroxene, clinopyroxene, and Fe-Ti oxides are commonly found as isolated crystals. Olivine is sometimes identified. Some of these crystals are angular. In addition, most of the samples include some cristobalite crystals.

4−2 Lapilli-size materials

The lapilli-size samples, ranging from 5 to 30 mm in size, can be grouped into three: Juvenile-A, Juvenile-B, and strongly altered types, as in the case of ash-size samples. On the basis of microscopic and BEI observations, it can be estimated that each type of lapilli was fragmented to produce the same types of ash samples. The isolated crystals in the ash samples must be also fragments of the lapilli samples (except for cristobalite).

(a) Juvenile-A type: This type consists of scoria and pumice, collected in November 2009 and April 2010, with a fresh and angular shape. The mineral assemblage is the same in all the samples: plagioclase, orthopyroxene, clinopyroxene, Fe-Ti oxides, and sometimes olivine in scoria (Fig. 5c). Their groundmass is intersertal in texture and composed mainly of plagioclase, with small amounts of pigeonite and magnetite, and light brown (scoria) or colorless (pumice) glass (Figs. 5a, 5c-d). On the BEIs, the

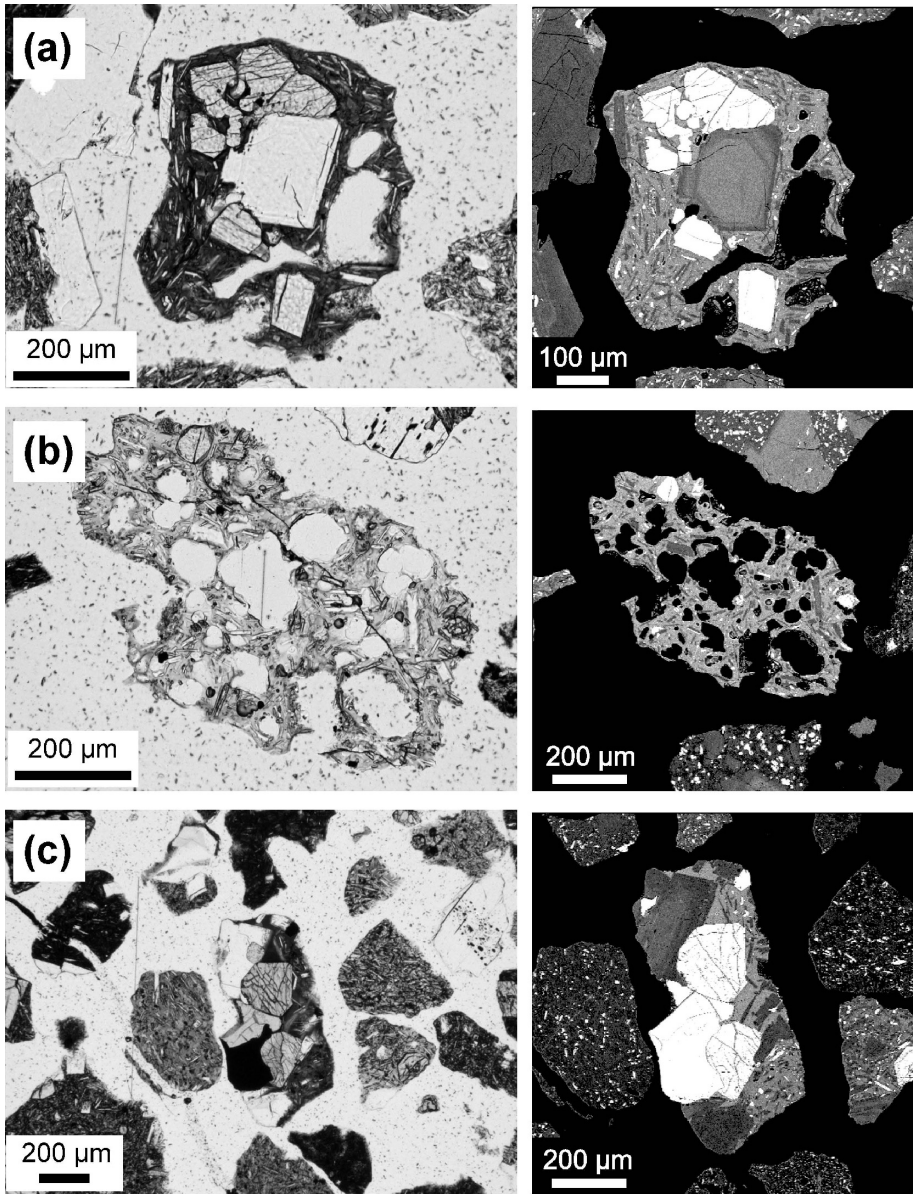

Fig. 4. Photomicrographs and back-scattered electron images (BEIs) of the representative component materials of the volcanic ash from Showa crater. (a) Scoria-type Juvenile-A, (b) pumice-type Juvenile-A with olivine phenocrysts (OL), (c) dense lithic-type Juvenile-A, (d) and (e) dense lithic-type Juvenile-B, (f) strongly altered (reddish lithic: arrow), and (g) strongly altered (silicified lithic). All Juvenile-A type materials can be distinguished from Juvenile-B by the higher brightness of matrix glass compared with plagioclase on the BEIs, whereas both materials appear similar features under microscopy.

matrix glass of this type is bright, and therefore the matrix glass is distinctive from plagioclase microlite (Figs. 5g-h). Considering these microscopic and BEI features, these materials can be considered as the juvenile products of each eruption.

(b) Juvenile-B type: Dense lithics (from all three eruptions) and some scoria and pumice (from the eruptions in April 2010 and June 2010) are classified under the Juvenile-B type. Most of the petrographical features of this type are nearly the same as those of the Juvenile-A type. However,

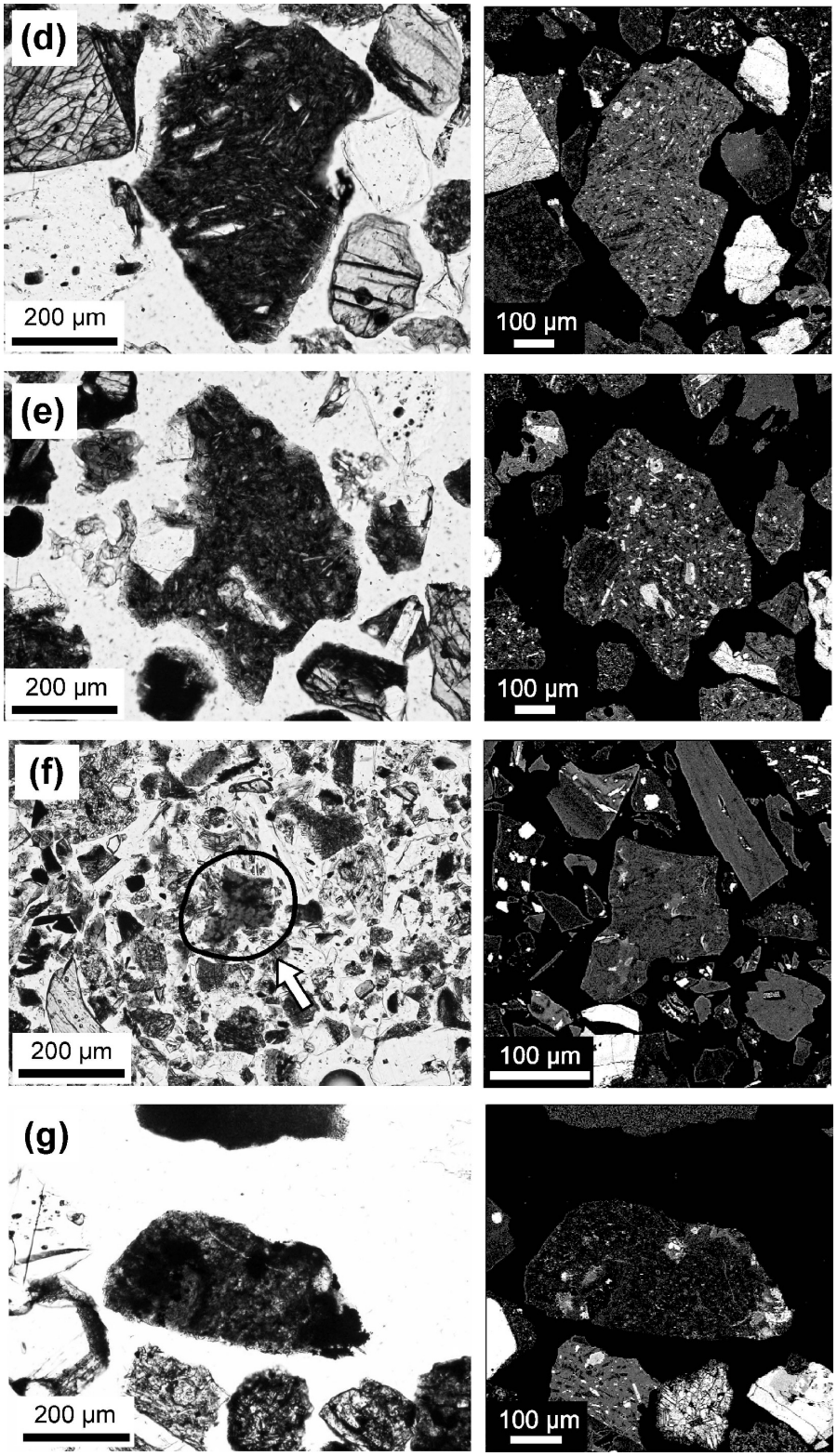

Fig. 4. Continued.

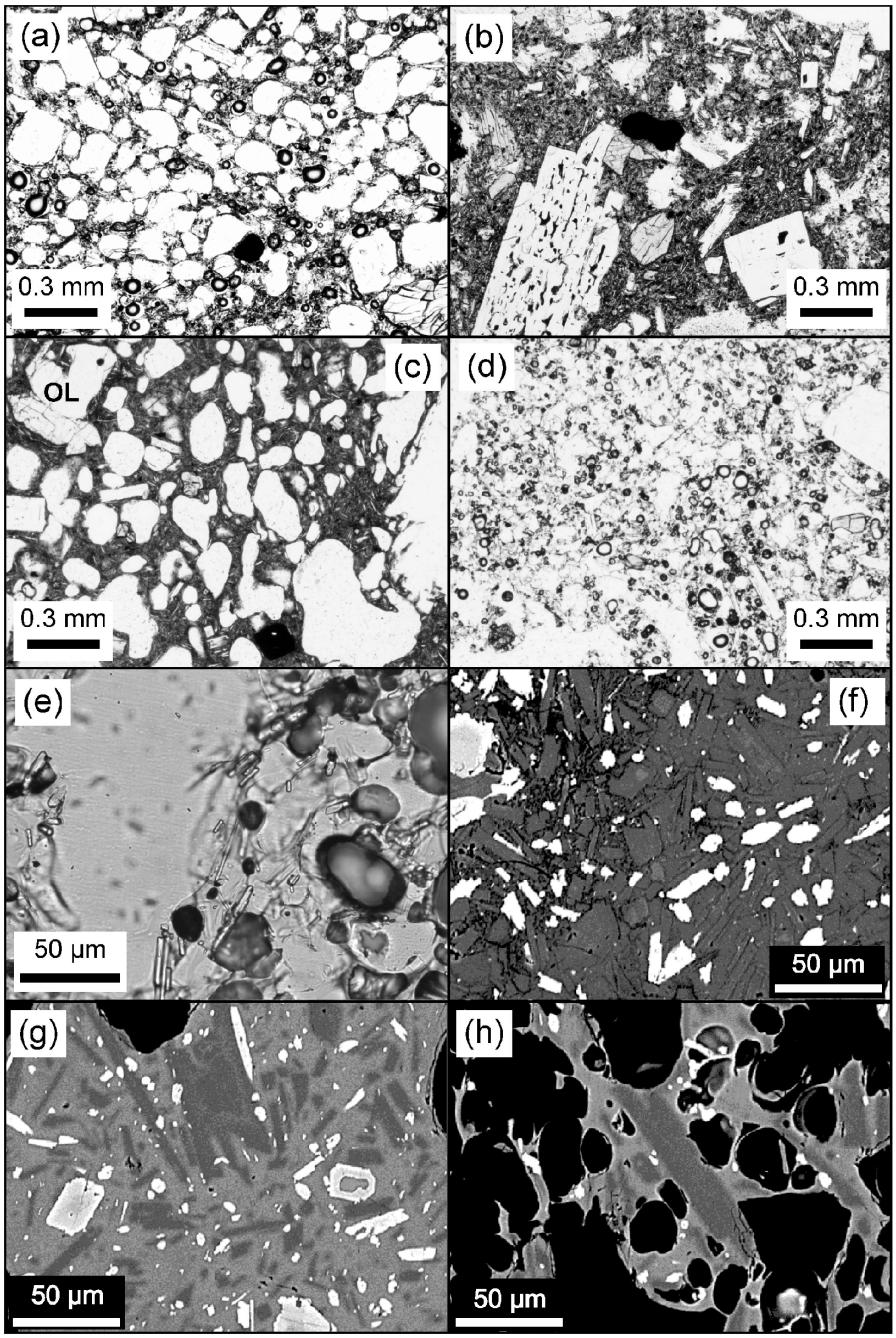

Fig. 5. Photomicrographs and back-scattered images (BEIs) of the lapilli-size materials during AD 2009 to 2010 from Showa crater. (a) and (e) Scoria of November 17, 2009 (Juvenile-A); (b) and (f) dense lithics of November 17, 2009 (Juvenile-B); (c) and (g) scoria of April 6, 2010 (Juvenile-A); (d) and (h) pumice of April 6, 2010 (Juvenile-A). The phenocrystic minerals consist of plagioclase, orthopyroxene, clinopyroxene, magnetite, and sometimes, olivine. The microlites are composed of plagioclase and small amounts of orthopyroxene and magnetite. On the BEIs, the matrix glass of dense lithics is darker than those of scoria and pumice and shows partial leaching (such as lacking of matrix interstitial glass). Therefore, most scoria and pumice are considered as juvenile materials, while dense lithics are probably accessory materials.

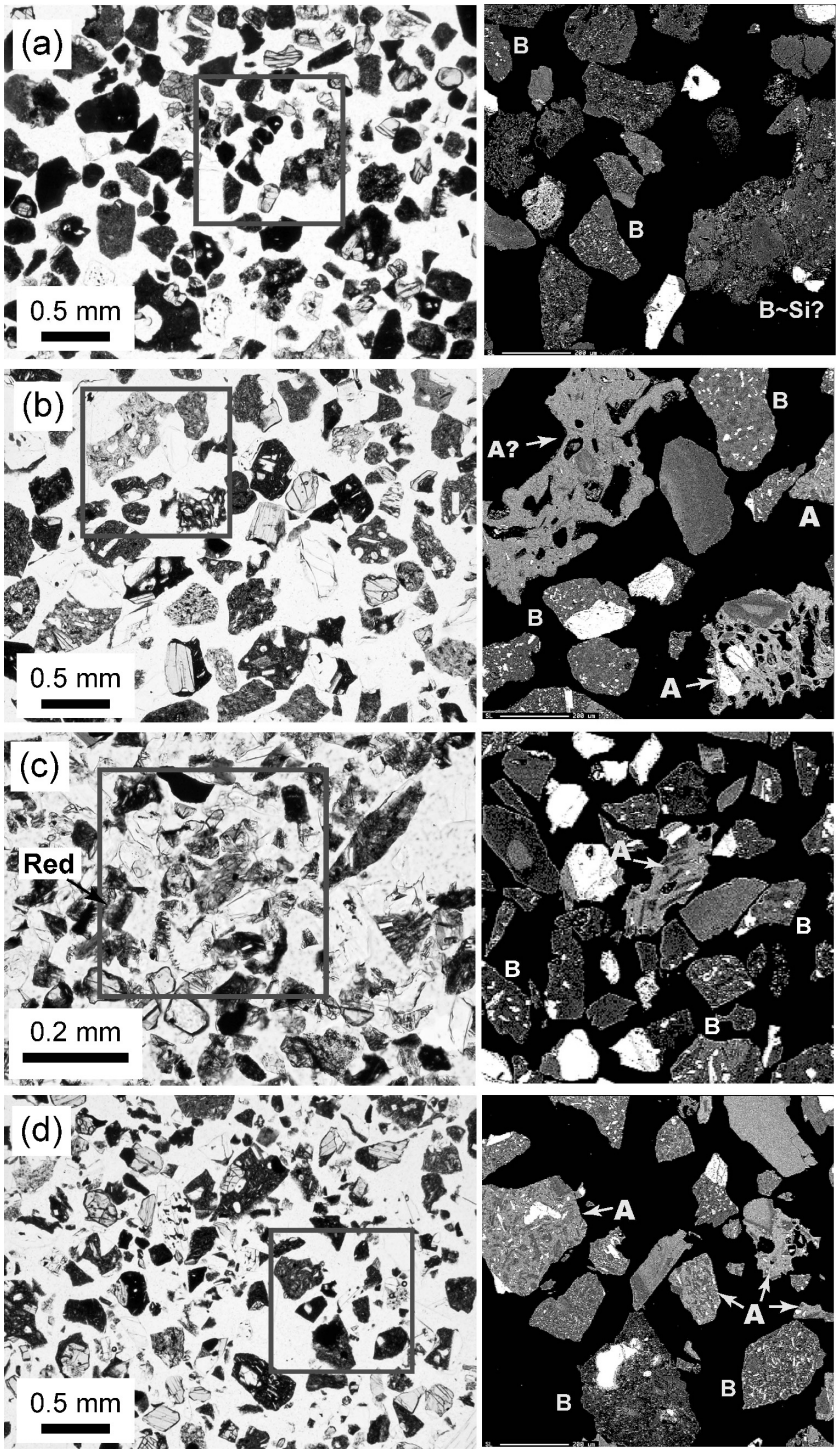

Fig. 6. Photomicrographs and BEIs of the volcanic ash at Showa crater from each period during AD 2006 to 2010. (a) March 2, 2009 (1st period); (b) February 19, 2010 (2nd period); (c) April 6, 2010 (3rd period); and (d) August 27, 2010 (4th period). Red squares in each photomicrograph shows the area of BEI. Abbreviations: A, Juvenile-A type; B, Juvenile-B type; Red, reddish lithic; and Si, silicified lithic.

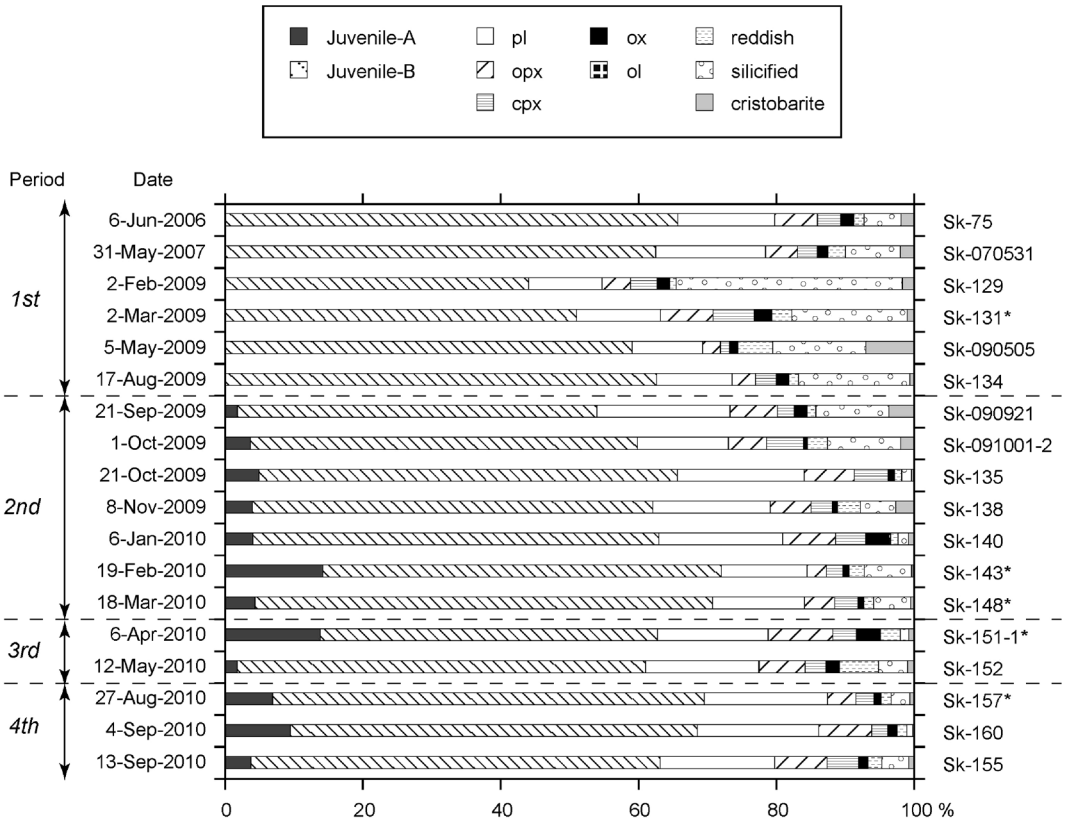

Fig. 7. The result of component analysis of the representative ash-size samples from Showa crater since AD 2006. Asterisk (*) shows the samples used for the bulk chemical analysis.

the matrix glass of Juvenile-B materials exhibits a dull color under microscope (Fig. 5b). In addition, the matrix glass is darker on the BEIs and shows partially leached features, such as lacking of matrix interstitial glass in some samples (Fig. 5f). Thus although Juvenile-B materials are slightly altered, their petrographical similarity to Juvenile-A materials suggests that they can be considered as magmatic materials related to the series of eruptive activities since AD 2006.

(c) Strongly altered type: This type consists of strongly altered lapilli. Such materials were observed only in April 2010 (Fig. 3b). They show a rounded shape and are reddish in color. Their matrix glass is glassy, showing a much darker in the BEIs. This type might be much older eruptive products not related to the activity since AD 2006.

4−3 Temporal variations of the petrographical features of volcanic ash

The volcanic ash from Showa crater show peculiar characteristics by following four periods: from June 2006 to August 2009; from September 2009 to March 2010; from April to May 2010; and from August to September 2010 (Figs. 6 and 7).

From June 2006 to August 2009 (the 1st period)

The volcanic ash ejected during this period is characterized by the absence of Juvenile-A type materials (Figs. 6a and 7) (although the samples from the activities in AD 2008 lacking). The ash comprises Juvenile-B-type materials (ca. 40−60 %), strongly altered materials (mainly silicified) (ca. 10−35 %), and isolated crystals (ca. 15−30 %). Olivine crystals are not found.

From September 2009 to March 2010 (the 2nd period)

The main components of the volcanic ash of this period are Juvenile-A and Juvenile-B types (ca. 50−70 %), and isolated crystals composed of plagioclase, orthopyroxene, clinopyroxene, Fe-Ti oxides, and a small amount of olivine (ca. 20−30 %) (Figs. 6b and 7). The strongly altered materials in this period are much fewer than the samples of the 1st period (ca. 5−20 %). Although Juvenile-A type materials are minor components in the ash of September 2009, their ratio in the eruptive ash had increased since late October 2009, from less than 5 % to 15 % (Fig. 7). The ratio of materials having a slightly smaller amount of microlites (Figs. 8a-b) seems to have increased in the ash samples ejected during the later phase of this period.

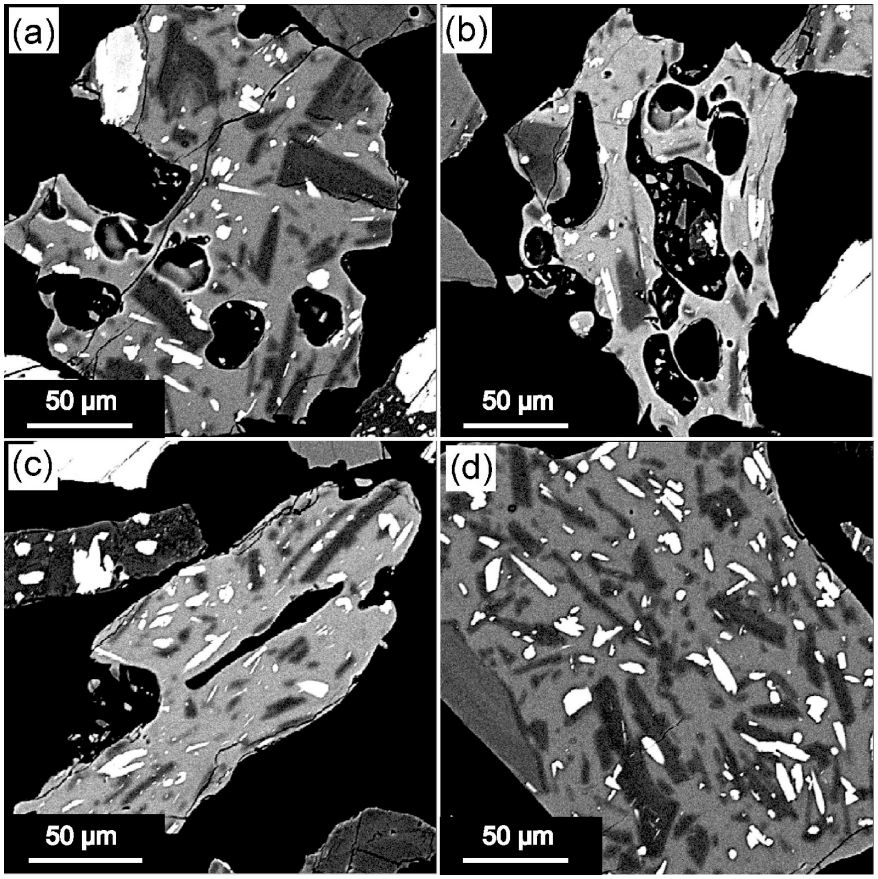

Fig. 8. The back-scattered electron images (BEIs) of the representative Juvenile-A type materials in the volcanic ash samples. (a) Volcanic glass from October 21, 2009 (2nd period, high-Si); (b) Volcanic glass from March 3, 2010 (2nd period: low-Si); (c) Volcanic glass from April 6, 2010 (3rd period: low-Si); and (d) Volcanic glass from September 13, 2010 (4th period: high-Si). The abundance of microlite of high-Si volcanic glass seems to be slightly larger than those of low-Si one.

From April 2010 to May 2010 (the 3rd period)

The volcanic ash of this period is characterized by the presence of more strongly altered materials: reddish lithics (Figs. 6c and 7). These ash-size samples consist mainly of Juvenile-A and Juvenile-B types (ca. 60 %), strongly altered materials (mainly reddish) (ca. 10−15 %), and isolated crystals (ca. 20−30 %). Olivine is sometimes present as an isolated crystal. The grain size of these ash samples is smaller than those in the earlier periods (Fig. 6c). Although many Juvenile-A type scoria and pumice with moderate microlite content are also found in the ash of April 2010 (ca. 14 %) (Fig. 8c), these components are much fewer in the volcanic ash of May 2010 (less than 3 %) (Fig. 7). In contrast, the ratio of reddish lithics in strongly altered materials increases in the sample of May 2010.

From August to September 2010 (the 4th period)

The proportion of Juvenile-A type materials increases from this period again (ca. 5−10 %) (Figs. 6d and 7). The groundmass of these materials exhibits moderate microlite content, slightly higher content than those of the 2nd and 3rd periods (Fig. 8d). The amount of strongly altered materials is less than those in the other periods (ca. 5−8 %). Olivine is sometimes present as an isolated crystal.

5. Geochemical features of the lapilli and volcanic ash

5−1 Whole-rock chemistry

The chemical compositions of the lapilli-size samples of Juvenile-A and Juvenile-B type materials show a narrow range of SiO_2 content (58.5−59.5 wt. %) irrespective of their type, such as scoria and lithic (Fig. 9). These samples are plotted on the areas of silica-poor end of the trends defined by the juvenile materials from Minamidake crater since AD 1955, consistent with our conclusion based on petrographical observation that both Juvenile-A and

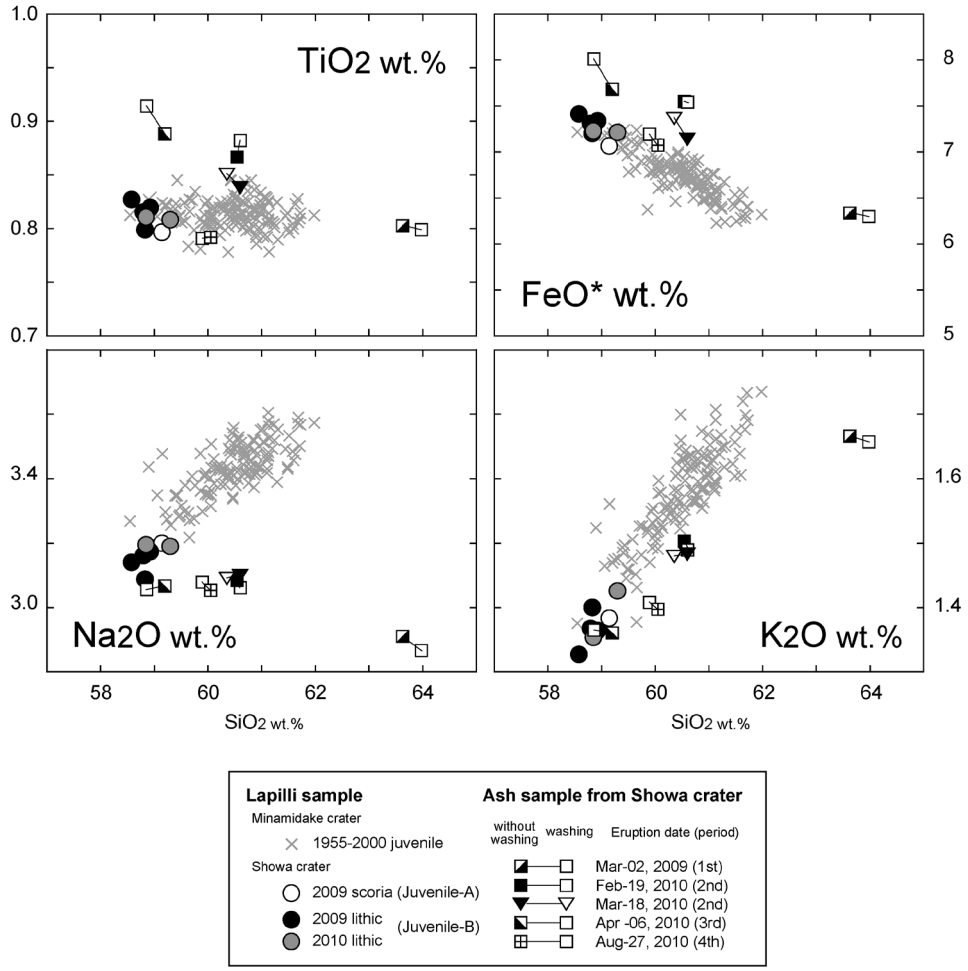

Fig. 9. Representative plots of oxides against SiO_2 for the whole-rock chemistry of the lapilli-size materials (Juvenile-A and Juvenile-B types) and volcanic ash since AD 2006 from Showa crater. The compositions of the 1955−2000 juveniles from Minamidake crater are also shown (Nakagawa *et al*., 2011). The lapilli-size samples from Showa crater exhibit the most mafic compositions among the juveniles since AD 1955, agreeing with the compositional trends in 20th-century juveniles. The compositions of the volcanic ash are clearly different from the trends found in juvenile lapilli.

Juvenile-B types of materials are essential (juvenile) ejecta in the activities since AD 2006.

We also determined the whole-rock chemical compositions of volcanic ash samples from five eruptions (March 2, 2009; February 19, 2010; March 18, 2010; April 6, 2010; and August 27, 2010). Although samples treated through different preparation methods (with or without washing with water) were analyzed, no obvious difference in chemical compositions due to the distinct preparation techniques was found. Compared with the whole-rock chemistry of lapilli-size juvenile clasts from AD 1955 to AD 2010, these samples displayed different trends in SiO_2 variation diagrams, showing higher TiO_2 and FeO* and lower Na_2O and K_2O contents (Fig. 9). Also, there is a clear compositional gap in SiO_2 content between the sample from March 2009 and the other samples. This might be consistent with the appearance of Juvenile-A type materials in addition to the decrease of strongly altered materials (silicified lithics) in the volcanic ash samples since September 2009 (Fig. 7).

5−2 Glass chemistry

The chemical compositions of volcanic glass in Juvenile-A type materials from the ash and lapilli-size samples, such as pumice, are dacitic (SiO_2＝67−72 wt.%; Fig. 10). The glass compositions in the volcanic ash are similar in each eruption, irrespective of the color and type of materials.

Focusing on temporal variation, the average of SiO_2

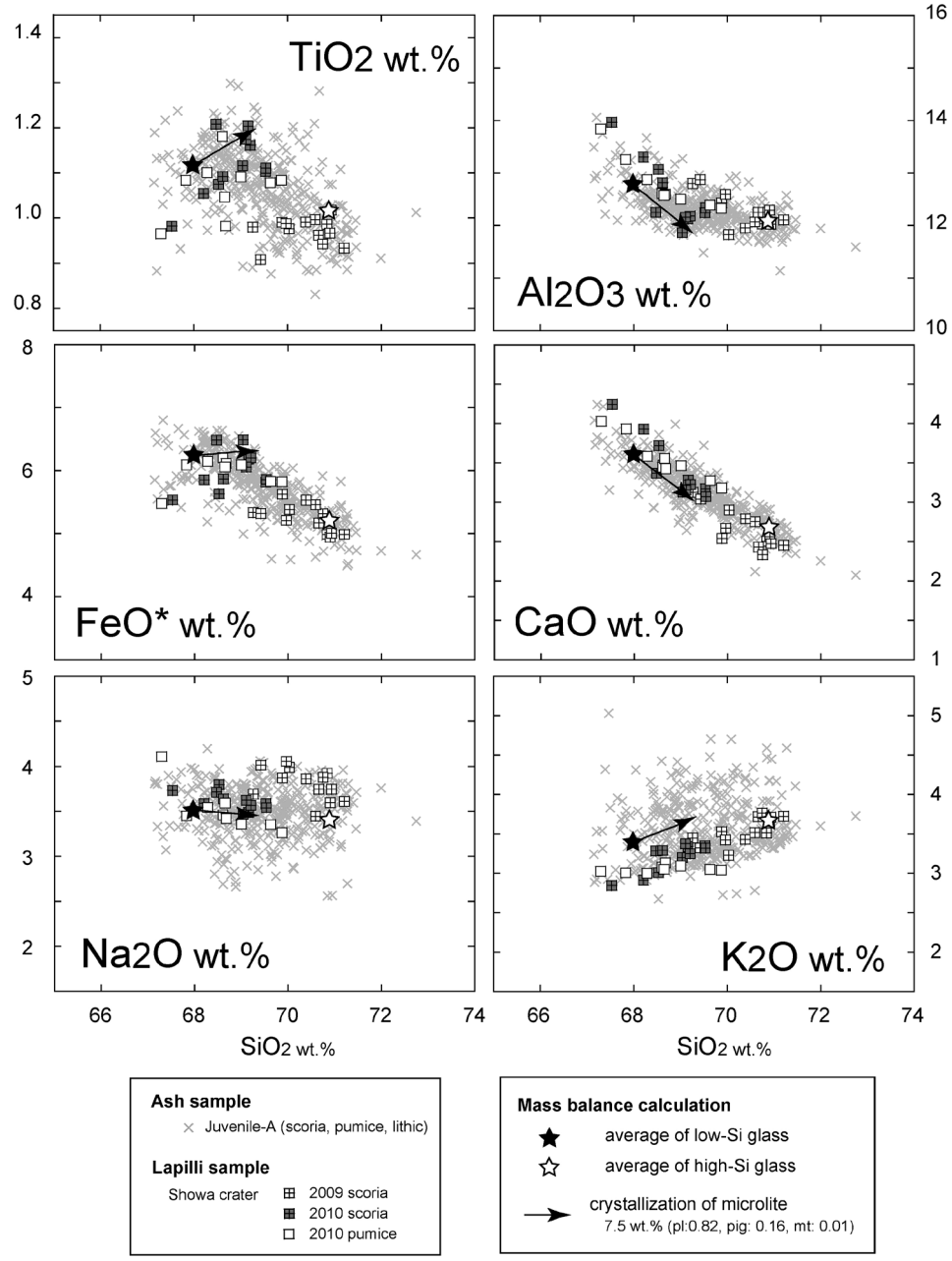

Fig. 10. Representative plots of oxides against SiO_2 for the matrix glass compositions of the juvenile materials in lapilli and volcanic ash from Showa crater. Arrows show the compositional trends of the results of mass balance calculations for the effect of microlite crystallinity on the basis of microlite modal compositions in the Juvenile-A type materials of the ash-size sample (plagioclase, pigeonite and magnetite: Table 3). Although there are no differences in size, the 2010 lapilli are slightly less silicic than the 2009 ones. Also, mass balance calculations cannot explain the compositional variations of matrix glass by the microlite crystallization, especially SiO_2, TiO_2 and FeO* contents.

content of glass compositions of each sample decreases from SiO_2＝71−70 wt.% in September 2009 to SiO_2＜69 wt.% in early April 2010 (Fig. 11). In contrast, the glass compositions of August to September 2010 seem to become more silicic with time. The average SiO_2 content of matrix glass of the lapilli-size juveniles of November 2009 and April 2010 is the same as those of juvenile materials in volcanic ash from eruptions in the same period. The matrix glass of the 2010 lapilli-size samples is more mafic than that of the 2009 samples.

6. Discussion

6−1 Comparison between the temporal variations of petrological features and geophysical data

Four periods defined by the temporal change in the proportion of the component types in volcanic ash would correspond to the monitoring data (Fig. 12). In the first period from June 2006 to September 2009, the level of eruptive activity had been lower than in the following periods, whereas inflation had gradually progressed, with small inflations and deflations occurring periodically. Since September 2009, remarkable inflation had been detected continuously, and the number of explosive eruptions and the weight of ejected volcanic ash increased with time until March 2010 (2nd period). This high level of eruptive activity until March 2010 would be consistent with the appearance of Juvenile-A-type materials during the period. In the third period from April to May 2010, explosive eruptions had almost ceased without ground deformation. The proportion of Juvenile-A type materials in volcanic ash also decreased. From June 2010 (4th period), the eruptive activity resumed with clear deflation. However, the number of explosive eruptions and the weight of ejected volcanic ash had become much less than those during the second period.

The temporal variations in the glass compositions are also consistent with the above division of eruptive activity. During the second period, the glass compositions gradually became less silicic, from SiO_2＝71.0 to 68.8 (in average). In the third period, the volcanic glass showed the most mafic composition (SiO_2＝68.7 wt.%). We were unable to investigate the temporal change in volcanic glass compositions from June 2010, but the four samples from August 2010 became slightly silicic again (Figs. 11 and 12).

The matrix glass composition reflects the crystallinity of microlite as well as the variations in the whole-rock composition and phenocryst mode of original magma. That is, differences in the crystallinity of the matrix affect compositional variations in the matrix glass (*e.g.*, Hammer *et al*., 2000). Thus, we examined the possibility of the effect of microlite crystallinity to matrix glass compositions on the basis of the observations. Indeed, as described above, especially in the 2nd period, the abundance of microlite decreases in the later samples (Fig. 8), and the silica content of matrix glass increases with time (Fig. 11). We performed mass balance calculations on the basis of the microlite modal compositions of representative high-Si and low-Si Juvenile-A type materials (Appendix 2), and we concluded that the matrix glass showed the compositional variations beyond the effect of microlite crystallinity (Fig. 10). For example, the difference of microlite crystallinity induces an increase of SiO_2 less than 2 wt.%, inconsistent with the range of matrix glass compositions (ca. 4 wt.%). On plots of Al_2O_3, CaO, Na_2O, and K_2O against SiO_2, the compositional trends by microlite crystallization might correspond to the measured data. On the other hand, TiO_2 and FeO* contents increase with increasing of SiO_2: this feature disagrees with the compositional variations of matrix glass. In addition, the sum of the squared residuals (R^2) shows low reproducibility in this calculation, and there are more than 10 % differences between the calculated and measured values on several elements (Table 3). Therefore, it is concluded that the compositional variations of matrix glass reflect the effect of mafic component, not being largely affected by the degree of microlite crystallinity.

In summary, the synchronized temporal changes in both the geophysical features of the eruptive activity and the petrological changes in the eruptive materials suggest that magmatic (in the chamber) and eruption (in the conduit) processes have temporally changed across the four periods since AD 2006. During each period, similar magmatic and eruption processes had continued, and had changed at the transition between periods. We note that during the 2nd period, magmatic and eruption processes might have changed gradually.

6−2 Deep processes during four episodes since AD 2006

It has already been indicated by previous studies that magma mixing was the main magmatic process during the historical activity on Sakurajima volcano: mafic magma had recharged into silicic magma (Miyasaka *et al*., 2010; Nakagawa *et al*., 2010, 2011; Yanagi *et al*., 1991). The whole-rock chemistry of the juvenile materials is consistent with the compositional variations in those from AD 1914 to AD 1999 (Fig. 9). Thus, it can be assumed that the eruptive magma since AD 2006 was also a magma-mixing product, as in the case of the AD 1914 and 1946 eruptions. If magma mixing has occurred, the temporal variations in the glass chemistry could be related to the mixing ratio between mafic and silicic end-member magmas as discussed above. If so, the temporal change in glass chemistry since the 2nd period suggests that the effect of the mafic component gradually increased during the 2nd and 3rd periods and then decreased in the 4th period. In other words, the temporal change in eruptive activity (*e. g.*, number of explosion and eruptive volume) might be related to the degree of the effect of the mafic component in the magma system. As mentioned before, each eruptive

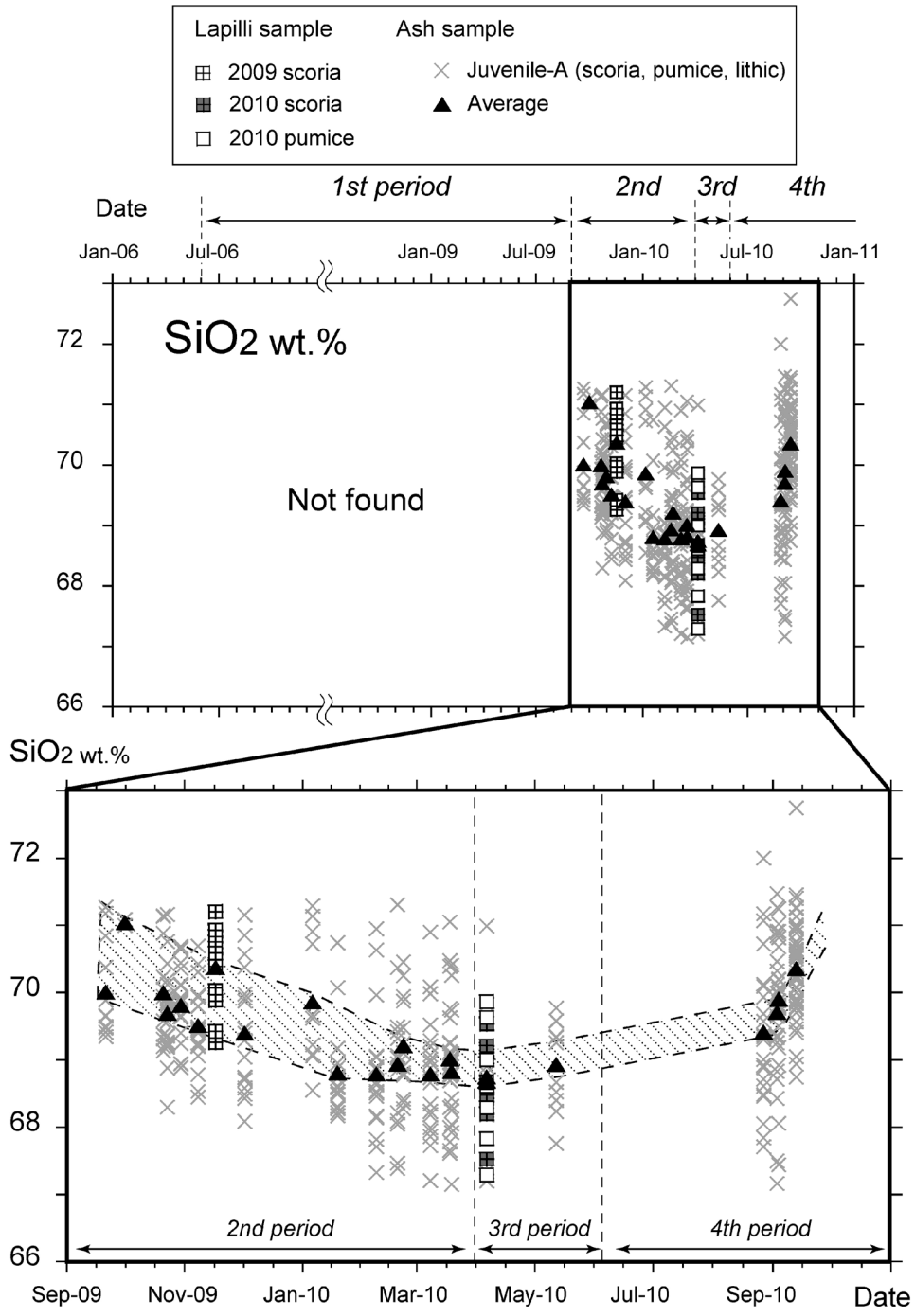

Fig. 11. Temporal change in the SiO_2 content of the matrix glass compositions of the Juvenile-A type materials in the volcanic ash and lapilli from Showa crater. The compositions of the lapilli-size samples also agree with the systematic variations of the volcanic ash. The temporal change in the glass compositions of the ash samples seems to be consistent with the eruptive episodes since AD 2006.

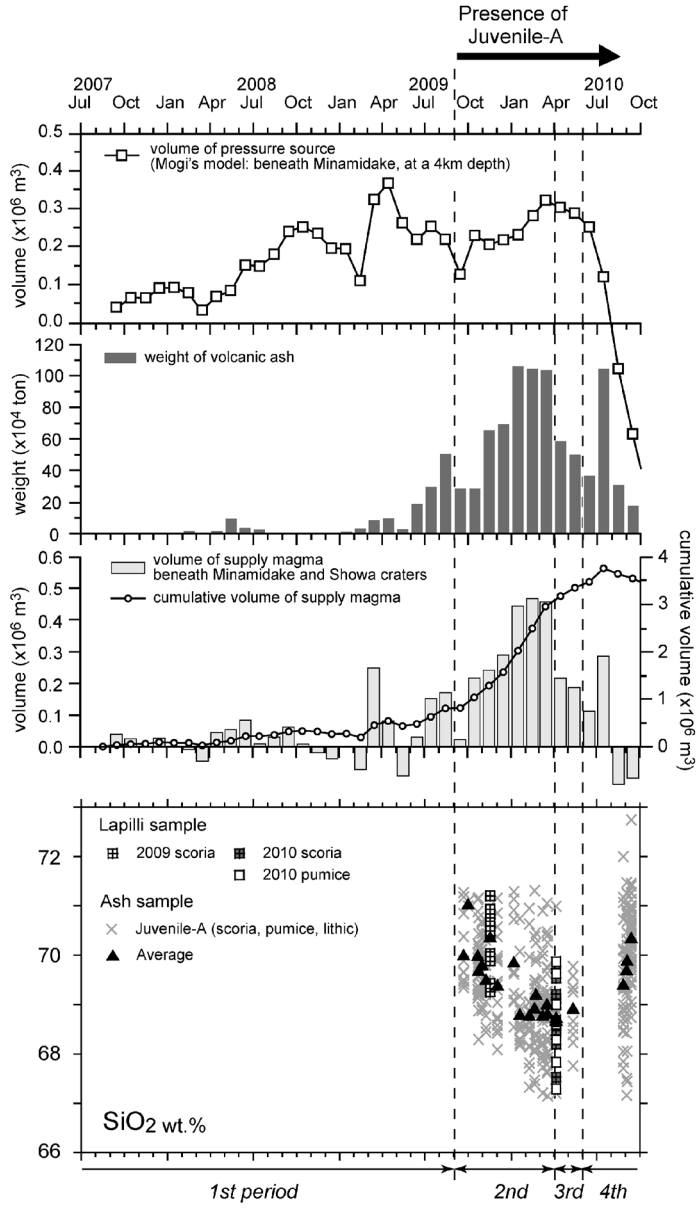

Fig. 12. Comparison between the magma supply rate beneath the Minamidake and Showa craters (Iguchi *et al*., 2013, in this issue) and the glass compositions of juveniles from Showa crater. The eruptive activity at Showa crater can be divided into four periods on the basis of the petrological features of the eruptive products as well as the geophysical data. The eruptive periods might be related to the injection of mafic magma. The 1st period: Because addition of mafic magma was small, andesitic magma was not supplied substantially, resulting in low eruptive activity without juveniles. The 2nd period: Mafic magma had significantly injected into magma system; therefore, a large amount of andesitic magma was supplied beneath the volcano, accompanied by remarkable inflation, an increase in the number of eruptions, and a decrease in the SiO_2 content of the volcanic glass of juveniles because of the increase of the effect of the mafic component. The 3rd period: The volcano had almost ceased erupting because the mafic magma recharge was much too small, and the supply volume of andesitic magma had decreased. The 4th period: The andesitic magma that had accumulated until the 3rd period had erupted, increasing the silica content of volcanic glass because of the absence of mafic magma recharge.

Table 3. Result of mass balance model for crystallization of microlite on the basis of modal compositions.

Mass balance calculation

		SiO_2	TiO_2	Al_2O_3	FeO*	MnO	MgO	CaO	Na_2O	K_2O	P_2O_5
Fractionated phese:7.5 wt.%		*6.2*Pl + 1.2*Pig + 0.1*Mt*									
Parent [a]	Ave. of low-Si	67.99	1.12	12.77	6.23	0.12	0.94	3.61	3.52	3.38	0.31
Daughter [a]	Ave. of high-Si	70.87	1.02	12.09	5.21	0.11	0.64	2.69	3.42	3.66	0.29
Result		69.10	1.18	11.99	6.30	0.12	0.76	3.11	3.47	3.64	0.34
	R	1.78	-0.17	0.11	-1.09	-0.01	-0.12	-0.42	-0.05	0.02	-0.04
	ΣR^2	4.58									
	R/Daughter	2.5	16.6	0.9	20.9	7.0	19.2	15.6	1.6	0.7	15.4
Fractionated minerals [b]											
	Plagioclase	55.56	0.00	27.02	0.97	0.00	0.12	10.99	5.01	0.34	0.00
	Pigeonite	52.80	0.33	0.90	22.11	0.72	18.64	4.41	0.10	0.00	0.00
	Magnetite	0.31	18.30	2.26	76.69	0.51	1.84	0.10	0.00	0.00	0.00

a: Data are taken from the average of high-Si and low-Si glass compositions from several samples.

b: The values are average of unpublished data of the microlites in the Juvenile-A type materials.

period from the 1st to the 3rd periods is characterized by a distinct mode of crustal deformation around the volcano. Thus, it is probable that the monitored deformation reflected the temporal change of the addition (injection) of mafic component to the magma plumbing system beneath the volcano.

In contrast, the eruptive activity has continued since June 2010 (4th period), whereas the crustal deflation has been monitored. In addition, the matrix glass of juvenile materials has become more silicic. These suggest that the addition of mafic component has decreased or ceased during the period. Thus, the eruptive activity during this period was not directly caused by the addition of mafic component but by a more open condition of the conduit, where already supplied silicic (andesitic) magma was easily tapped to produce the explosive activities. This explanation might be consistent with the much lower level of eruptive activity in the 4th period than that in the 2nd period.

Based on long-term geophysical monitoring, especially geodesy, magma accumulation has continued beneath the Aira caldera adjacent to Sakurajima volcano (Eto *et al*., 1997; Iguchi *et al*., 2008a; Kamo, 1978; Kamo *et al*., 1997). It has also been suggested that part of the accumulated magma had moved into the volcano during previous eruptive activity, resulting in the frequent explosive eruptions from AD 1955 to the end of the 20th century (Kamo, 1978). In addition, the whole-rock compositions of the 2009−2010 juvenile materials are concordant with the compositional variations in juvenile materials from the 20th-century activity (Fig. 9). Therefore, it is inferred that the andesitic magma system since AD 2006 is nearly the same as that during the 20th activity and that andesitic magma has been supplied from the inflated pressure source beneath the Aira caldera to Sakurajima volcano since AD 2006.

However, the previous model based on geophysical monitoring did not consider the effect of the mafic component on the andesite magma migrating from the Aira caldera toward Sakurajima volcano. In order to re-evaluate the geophysical data and to revise the model of the magma plumbing system of the volcano, additional petrological and geochemical investigations for the rocks from recent eruptive activity especially after AD 1970s must be carried out, because dense and excellent geophysical monitoring has continued until now.

6−3 Evaluation of the chemical compositions of volcanic ash

The chemical compositions of volcanic ash are easily determined and must be correlated with the features of the juvenile materials. However, the whole-rock composition of volcanic ash is usually different from that of adequate-size juvenile materials. This is because the ratio of mineral to melt in volcanic ash is different from that in the derived magma due to the separation of mineral and melt by fragmentation and transportation. In addition, the ash sample often includes materials that are not juveniles (*e.g.*, altered rocks and basement sediments). Even though these problems, we tentatively evaluate the bulk chemical compositions of volcanic ash from several eruptions in order to develop conventional methods of monitoring of eruptive materials.

Comparing the whole-rock chemical compositions of ash samples and lapilli-size ones (Juvenile-A and Juvenile-B type materials), the ash samples are higher in SiO_2, TiO_2, FeO*, and MgO, and lower in Na_2O, K_2O, and Al_2O_3 contents. This suggests that the compositional differences between lapilli-size and ash-size samples are related to the separation of crystals and melt by fragmentation. The isolated crystals in the volcanic ash are plagioclase, orthopyroxene, clinopyroxene, Fe-Ti oxides, and some-

times olivine. If any combinations of these isolated crystals accumulate, the whole-rock composition of volcanic ash becomes lower in silica content. Thus, higher SiO_2 content in the whole-rock compositions of the volcanic ash would be produced by the accumulation of the strongly altered materials (silicified lithics and cristobalite).

Among the ash-size samples, the chemical compositions of the sample from the 1st period show higher SiO_2 and lower Na_2O contents than those of juvenile materials, probably reflecting a dominant proportion of altered materials, especially silicified lithics (Fig. 7). The SiO_2 contents of the volcanic ash from the 2nd to the 4th periods are lower than that in the 1st period, consistent also with the microscopic observation that these ash samples are mainly composed of Juvenile-A and -B type materials with less amounts of strongly altered materials than the samples in the 1st period (Figs. 7 and 9). Although the change in SiO_2 content of ash samples from the 2rd to 4th periods might reflect the proportion of components of silicified lithics, we are unable to evaluate because of the paucity of the data (only 5 samples).

In summary, there exists a discrepancy in chemical composition between the coarse juvenile materials and ash samples even in the 2nd to the 4th periods, when Juvenile-A type materials were ejected (Fig. 9). Even so, the large differences in the chemical compositions of ash samples between the 1st and the other periods can be recognized. The difference of the 1st period from the others is consistent with the existence of a large amount of silicified lithics in the ash samples. Interestingly, the proportion of silicified lithics in the ash samples from Showa crater during AD 2006 to September 2010 correlates with the presence of Juvenile-A type materials: the ash samples in the 1st period that include more silicified lithics are in the absence of Juvenile-A types (Fig. 7). Therefore, the silica content of the whole-rock compositions of ash samples can be a good index to identify the eruption type: the presence or absence of magmatic materials related to magma in each eruption. Although we used only five samples in this examination and the components of volcanic ash samples might depend on their grain size (Miyagi, unpublished data), at least, the chemical analysis of ash samples might become a tool for monitoring in ongoing eruptions at Sakurajima volcano.

7. Concluding remarks

We revealed the petrological features of the dated volcanic ash and lapilli-size materials since AD 2006 collected from Showa crater. Also, we revealed the relationships between the petrological features of eruptive products and the geophysical data set, and indicated the effect of the magma migration (or supply) on the mode of eruption in the activity at Showa crater since AD 2006. For evaluation of future eruptive activity, it is necessary to combine the geophysical and petrological observations in detail. The eruptive activity at Sakurajima volcano is ongoing, and therefore, we must continue the petrological monitoring of the eruptive materials.

Acknowledgements

We express our gratitude to T. Kobayashi and H. Miyamachi for helping in the collection of samples. We wish to thank H. Nomura and K. Nakamura for preparing the thin sections. We appreciate to H. Sato and I. Miyagi for valuable and constructive comments. We also thank M. Ban for editing our paper.

References

Eto, T., Takayama, T., Yamamoto, K., Hendrasto, M., *et al*. (1997) Re-upheaval of the ground surface at the Aira caldera −December 1991～October 1996-. *Annuals of Disas. Prev. Res. Inst., Kyoto Univ.*, **40**, 49−60 (in Japanese with English abstract).

Fukuyama, H. and Ono, K. (1981) *Geological map of Sakurajima volcano, 1 : 25000*. Tsukuba: Geological Survey of Japan (in Japanese with English abstract).

Hammer, J.E., Cashman, K.V. and Voight, B. (2000) Magmatic processes revealed by textural and compositional trends in Merapi dome lavas. *J. Volcanol. Geotherm. Res.*, **100**, 165−192.

Iguchi, M. (2010) Eruptive activity of Sakurajima volcano during the period from February 2009 to May 2010. In *Study on preparation process of volcanic eruption based on integrated volcano observation 2009*, Sakurajima Volcano Research Center, 1−8 (in Japanese with English abstract).

Iguchi, M., Takayama, T., Yamazaki, T., Tada, M., *et al*. (2008a) Movement of magma at Sakurajima volcano revealed by GPS observation. *Annuals of Disas. Prev. Res. Inst., Kyoto Univ.*, **51**, 241−246 (in Japanese with English abstract).

Iguchi, M., Tameguri, K. and Yokoo, A. (2008b) Volcanic activity of Sakurajima volcano during the period from 1997 to 2007. In *10th Joint Observation of Sakurajima Volcano*, Sakurajima Volcano Research Center, 1−18 (in Japanese).

Iguchi, M., Ueki, S., Ohta, Y., Nakao, S., Sonoda, T., Takayama, T. and Ichikawa, N. (2010) GPS observation after the beginning of eruptive activity at Showa crater of Sakurajima volcano. In *Study on preparation process of volcanic eruption based on integrated volcano observation*, Sakurajima Volcano Research Center, 47−53 (in Japanese with English abstract).

Iguchi, M., Ohta, Y., Ueki, S., Tameguri, T., Sonoda, T., Takayama, T. and Ichikawa, N. (2011) Evaluation of volcanic activity of Sakurajima volcano in 2010. *Annuals of Disas. Prev. Res. Inst., Kyoto Univ.*, **54**, 171−184 (in Japanese with English abstract).

Iguchi, M., *et al*. (2013) Volcanic activity and the mechanism of explosive eruptions at Showa crater of Sakurajima volcano. *Bull. Volcanol. Soc. Japan*, (in Japanese with English abstract, in this issue).

Kamo, K. (1978) Some phenomena before the summit eruptions at Sakura-zima volcano. *Bull. Volcanol. Soc. Japan*,

23, 53–64 (in Japanese with English abstract).

Kamo, K., Iguchi, M. and Ishihara, K. (1997) Inflation of volcano Sakurajima detected by automated monitoring system of GPS network. Program manual '97 IUGG IAG International Symposium on Current Crustal Movement and Hazard Reduction in East Asia and South-east Asia November 4–7, 1997, Wuhan, China, 38.

Kobayashi, T. (1982) Geology of Sakurajima volcano: a review. *Bull. Volcanol. Soc. Japan*, **27**, 277–292 (in Japanese with English abstract).

Kobayashi, T. and Ishihara, K. (1988) Historic eruptions and recent activities. In *Guide Book for Sakurajima Volcano*, Kagoshima International Conference on Volcanoes, Kagoshima, Japan, July 19–23, 1988, 7–11.

Miyagi, I. and Tomiya, A. (2002) Feature of the Miyakejima 2000 ash particles and identification of the essential material. *Bull. Volcanol. Soc. Japan*, **47**, 27–31 (in Japanese with English abstract).

Miyagi, I., Itoh, J., Shinohara, H., Kagoshima Observatory and Japan Meteorological Agency (2010) Re-activation process of Showa volcanic vent at Sakura-jima volcano in 2008: evidence from volcanic ash. *Bull. Volcanol. Soc. Japan*, **55**, 21–39 (in Japanese with English abstract).

Miyasaka, M., Togashi, Y., Nakagawa, M. and Kobayashi, T. (2010) Magmatic system of historic eruptions of Sakurajima volcano. *Abstracts*, Japan Geoscience Union Meeting 2010, SVC063–13.

Nakagawa, M., Matsumoto, A., Miyasaka, M. and Iguchi, M. (2011) Change of mode of eruptive activity and the magma plumbing system of Sakurajima volcano since the 20th century. In *Study on preparation process of volcanic eruption based on integrated volcano observation 2010*, Sakurajima Volcano Research Center, 85–94 (in Japanese with English abstract).

Nakagawa, M., Miyasaka, M., Iguchi, M. and Nogami, K. (2010) Magma related to the eruptive activity of Sakurajima volcano since 2006. *Abstracts*, Japan Geoscience Union Meeting 2010, SVC063–15.

Shimano, T., Yokoo, A., Iguchi, M. and Miki, D. (2010) Grain size monitoring of ashfall from Showa crater by time series sampling at Sakurajima volcano. *Abstracts,* Volcanol. Soc. Japan Fall Meeting 2010, 41.

Yanagi, T., Ichimaru, Y. and Hirahara, S. (1991) Petrochemical evidence for coupled magma chambers beneath the Sakurajima volcano, Kyushu, Japan. *Geochem. J.*, **25**, 17–30.

Yokoo, A., Tameguri, T. and Iguchi, M. (2009) Swelling of a lava plug associated with a vulcanian eruption at Sakurajima volcano, Japan, as revealed by infrasound record: case study of the eruption on January 2, 2007. *Bull. Volcanol.*, **71**, 619–630.

Appendix 1, 2

Appendix 1. Representative matrix glass compositions of Juvenile-B type and reddish lithics in the volcanic ash samples.

Grain No.	Sk-131-B2	Sk-143-B2	Sk-151-B1	Sk-155-B1	Sk-152-R1	Sk-152-R2
Type	B-type	B-type	B-type	B-type	Reddish	Reddish
Glass composition (wt.%, EPMA)						
SiO_2	71.98	77.74	72.98	74.11	68.81	72.59
TiO_2	0.89	0.66	0.94	0.98	0.70	0.92
Al_2O_3	13.01	11.53	11.58	11.80	13.99	12.35
FeO*	4.03	2.64	4.66	3.93	4.20	3.40
MnO	0.10	0.07	0.06	0.03	0.12	0.08
MgO	0.45	0.19	0.44	0.16	1.03	0.59
CaO	2.33	1.12	2.07	1.52	4.13	2.16
Na_2O	3.70	3.80	3.61	3.56	4.42	3.25
K_2O	3.37	4.07	3.96	4.52	1.97	4.08
P_2O_5	0.23	0.10	0.29	0.38	0.23	0.28
Total	100.09	101.91	100.59	100.98	99.59	99.71

Appendix 2. Modal compositions of microlite of the matrix with high-Si and low-Si glass (Juvenile-A types).

high-Si		(μm^2)				*low-Si*		(μm^2)			
Date	Grain No.	pl	pig	mt	glass	Date	Grain No.	pl	pig	mt	glass
21-Sep-2009	gl-2	1657	452	10	3881	8-Mar-2010	gl-1	2767	305	0	4927
	gl-5	1456	527	22	6995		gl-5	2508	684	0	8183
	gl-14	2130	529	124	6031		gl-2	1677	770	19	5534
1-Oct-2009	gl-5	8195	1876	259	16669		gl-9	1193	675	213	5683
	gl-6	10377	1712	36	18875		gl-12	6325	1558	75	14072
21-Oct-2009	gl-1	559	313	79	4050		gl-17	1815	833	0	9575
	gl-6	4198	3242	113	8447		gl-21	2478	481	0	4597
	gl-7	10865	2697	193	20245	18-Mar-2010	gl-1	7559	2085	45	15501
	gl-11	7233	2507	65	13887		gl-9	3596	1100	61	11646
	gl-20	547	410	7	2036		gl-10	11557	4888	640	44915
13-Sep-2010	gl-8	12275	3410	233	21082		gl-13	1095	0	0	2905
	gl-9	2818	588	22	6572		gl-14	5562	1454	54	9931
	gl-11	3217	1028	181	7128	6-Apr-2010	gl-3	799	183	0	3018
	gl-15	2743	1445	0	6812		gl-8	805	331	0	2778
	gl-25	1744	477	25	6754		gl-9	1527	489	0	3984
	gl-27	3376	1157	131	6336		gl-10	1636	417	101	3845
							gl-12	2540	1444	165	9850
	Total (μm^2)	73389	22371	1499	155800		gl-13	1740	1164	0	9594
	Total area (mm^2)				0.253		gl-22	917	1078	0	4987
							Total (μm^2)	58097	19940	1374	175524
							Total area (mm^2)				0.255

Modal composition*		pl	pig	mt	glass			pl	pig	mt	glass
high-Si	vol.%	29.0	8.8	0.6	61.6	low-Si	vol.%	22.8	7.8	0.5	68.9
	wt.%	30.3	11.7	1.2	56.8		wt.%	24.1	10.5	1.1	64.3

*: Densities of minerals are assumed as follows: plagioclase, 2.6; pigeonite, 3.3; and magnetite, 5.2.

(Editorial handling Masao Ban)

桜島火山，2006～2010 年の昭和火口噴出物の岩石学的特徴の時間変化

松本亜希子・中川光弘・宮坂瑞穂・井口正人

九州南部に位置する桜島火山は，2006 年 6 月に昭和火口における噴火活動を再開した．我々は，2006 年 6 月～2010 年 9 月に噴出した火山灰及び火山礫について岩石学的特徴を明らかにし，マグマの特徴とその時間変化，そして噴火活動との関係を検討した．その結果，2006 年以降の昭和火口の活動が以下の 4 つの活動期に区分されることが明らかになった．第 1 期（2006 年 6 月～2009 年 8 月）: この期間は，爆発的噴火が少なく，小さな山体膨張・収縮が繰り返された．噴出物中に本質物は認められない．第 2 期（2009 年 9 月～2010 年 3 月）: この期間は，爆発的噴火の頻度・規模ともに大きくなり，明瞭な山体膨張が継続した．噴出物中には本質物（スコリア・軽石）が認められる．火山礫の全岩化学組成は，1955 年以降の噴出物の組成トレンドと調和的で，且つ最も苦鉄質な組成を示す (SiO_2＝58.5−59.1 wt.%)．これは，桜島火山では 1955 年以降同じマグマ系が活動しており，珪長質マグマに苦鉄質マグマが注入していることを示唆している．また，火山灰中の本質物の量比は時間とともに増加し，その石基ガラス組成は時間とともに SiO_2 量が減少している．従って，第 2 期では，噴出マグマにおける苦鉄質マグマの割合の増加が活動規模を拡大させていると考えられる．第 3 期（2010 年 4 月～5 月）: この期間は噴火頻度が極端に低下し，山体膨張もほぼ停止した．噴出物中に本質物は認められるが，その量は少なく，変質岩片が増加する．第 4 期（2010 年 6 月～2010 年 9 月）: この期間になると，明瞭な山体収縮が始まり，火山爆発も再び活発化した．噴出物中に本質物が多く認められるようになるが，その石基ガラス組成はやや珪長質であることから，この時期の噴出マグマは苦鉄質マグマの影響が小さいと言える．つまり，2006 年以降の桜島火山では，マグマ系に注入する苦鉄質マグマそのものが噴出しているのではなく，既に火山下に供給されている珪長質マグマが主体となって活動していると考えられる．